

Postprint of: Koziel S., Pietrenko W., Robust Parameter Tuning of Antenna Structures by Means of Design Specification Adaptation, IEEE TRANSACTIONS ON ANTENNAS AND PROPAGATION (2021), pp. 1-7, DOI: [10.1109/TAP.2021.3083792](https://doi.org/10.1109/TAP.2021.3083792)

© 2021 IEEE. Personal use of this material is permitted. Permission from IEEE must be obtained for all other uses, in any current or future media, including reprinting/republishing this material for advertising or promotional purposes, creating new collective works, for resale or redistribution to servers or lists, or reuse of any copyrighted component of this work in other works.

Robust Parameter Tuning of Antenna Structures by Means of Design Specification Adaptation

Slawomir Koziel, *Senior Member, IEEE*, and Anna Pietrenko-Dabrowska, *Senior Member, IEEE*

Abstract—Parameter tuning through numerical optimization has become instrumental in the design of high-performance antenna systems. Yet, practical optimization faces several major challenges, including high cost of massive evaluations of antenna characteristics, normally involving full-wave electromagnetic (EM) analysis, large numbers of adjustable variables, the shortage of reasonable initial solutions in the case of topologically complex structures, and multimodality of the objective function landscapes. The last two reasons foster the employment of global search routines, which might be prohibitively expensive. This paper proposes a novel procedure for efficient and reliable antenna optimization by means of design specification adaptation. By using appropriate selection criteria and the predictions from a linear expansion model, the ability of improving the current design is verified, and—in the case of a negative outcome—performance requirements are temporarily relaxed. The adjustment is carried out prior to each iteration of the optimization process with the specifications eventually converging to their original levels. The algorithm is intended to improve the efficacy of local optimizers if the target operating frequencies of the structure at hand are severely misaligned with respect to those at the available initial design. This eliminates the need for global routines, and greatly enhances the robustness of the search process, as demonstrated using several antenna structures optimized under different scenarios.

Index Terms—Antenna design; parameter tuning; EM-driven optimization; design specification adaptation; multi-band antennas.

I. INTRODUCTION

Simulation-driven parameter tuning has become ubiquitous in the design of contemporary antenna structures. As performance specifications become increasingly stringent, which is in a large part dictated by the needs of the emerging application areas (5G communications [1], medical imaging [2], internet of things [3], or wearable devices [4]), their fulfillment fosters the development of topologically complex structures described by many parameters that require meticulous tuning. At the same time, implementation of functionalities such as multi-band operation [5], circular polarization [6], band notches [7], or spatial diversity (e.g., MIMO technology [8]), requires handling of various antenna characteristics (axial ratio [9], isolation [10], gain [11]), as well

as constraints, e.g., in the case of compact realizations [12]. Controlling multiple parameters and performance figures through numerical optimization is a challenging endeavor, yet imperative to render high-performance designs. The primary bottleneck is high cost of repetitive EM analyses entailed by both local and global search procedures. To alleviate this difficulty, a number of techniques have been devised, including algorithmic approaches (adjoint sensitivities [13], sparse Jacobian updates [14]), surrogate-based methods involving both physics-based [15], [16] (e.g., space mapping [17], response correction [18], cognition-driven design [19]), and data-driven models [20], [21] (e.g., kriging [22], support vector regression [23]), or machine learning methodologies [24], [25]. Another possibility, partially related to the physics-based approaches, is the employment of variable-fidelity simulations, e.g., by means of co-kriging [26], multi-fidelity algorithms [27], or supervised learning [28].

In many practical situations, ensuring reliability is of an even higher priority than reducing the computational complexity. When carrying out parameter tuning, e.g., to re-design an antenna for different operating frequencies or material parameters of a dielectric substrate, or boosting the performance of a compact device after introducing geometrical alterations, the available initial solution may be too far away from the optimum, especially in terms of allocating the operating frequencies. This makes local routines prone to a failure, and promotes defaulting to global methods, which should only be used as the last resort due to their excessive CPU costs. The methods mentioned in the previous paragraph are mostly oriented towards the improvement of the computational efficiency of the search process, but not directly addressing its robustness [13]-[25]. On the other hand, accelerated versions of globalized algorithms (e.g., surrogate-assisted nature-inspired procedures [29], [30]) are severely limited in terms of the dimensionality of the parameter space they can handle [31], [32], which is typically way below the number of adjustable variables inherent to contemporary devices. The problem is further exacerbated by nonlinearity of antenna characteristics.

This paper proposes a technique for improving the reliability of the optimization procedures by introducing adaptation of design specifications. Our methodology adjusts the objectives based on appropriately quantified misalignments between the

The manuscript was submitted on December 23, 2020. This work was supported in part by the Icelandic Centre for Research (RANNIS) Grant 217771, and by Gdańsk University of Technology Grant DEC-41/2020/IDUB/I.3.3 under the Argentum Triggering Research Grants program - ‘Excellence Initiative - Research University’.

S. Koziel is with Engineering Optimization and Modeling Center of Reykjavik University, Reykjavik, Iceland (e-mail: koziel@ru.is); A. Pietrenko-Dabrowska and also S. Koziel are with Faculty of Electronics, Telecommunications and Informatics, Gdansk University of Technology, 80-233 Gdansk, Poland.

required operating frequencies/bandwidths and those of the current design. The adjustments are made in the course of the optimization run, eventually converging to the original targets. For the sake of validation, the proposed mechanism is coupled with the gradient-based optimization routine, and demonstrated to significantly improve the robustness of the search process in several ways: (i) making the successful execution of the optimization procedure less dependent on the quality of the initial design, (ii) enabling re-design of antenna structures in broad ranges of operating frequencies using local algorithms, (iii) eliminating the need for employing global search procedures, (iv) eliminating the need for using sophisticated algorithmic solutions such as surrogate modeling or machine learning methods. The numerical experiments carried out using three antenna structures, a single-, dual-, and triple-band ones fully corroborate these features, and make the presented approach a viable alternative for existing optimization techniques for solving more demanding optimization tasks.

The major novelties and technical contributions of this work include: (i) conceptual development of the design specification management scheme, (ii) implementation of the optimization framework combining local gradient-based search with automated specification adjustment, (iii) comprehensive exposition of the search process reliability improvement in terms of reducing sensitivity to the initial design quality, (iv) demonstrating the efficacy of the proposed procedure in handling severe operating frequency misalignments (initial versus target) through local search.

The remaining part of the paper is organized as follows. Section II introduces the proposed design specification management methodology and places it in the context of local (gradient-based) design optimization of antenna structures. Section III provides comprehensive validation of the developed framework as well as benchmarking against conventional formulation of the parameter tuning tasks involving fixed specifications. The numerical experiments emphasize the importance of the adaptive adjustment of the target operating frequencies in the course of the optimization run, and the benefits in terms of handling challenging design scenarios. Section IV concludes the work.

II. ROBUST OPTIMIZATION USING DESIGN SPECIFICATION ADJUSTMENT

This section formulates the proposed design specification management strategy that aims at improving the robustness of the antenna optimization process. Although it is generic, for the sake of illustration, it is combined with the gradient-based algorithm briefly outlined in Section II.C. The overall optimization framework is summarized in Section II.D.

A. Design Specification Management for Reliable Antenna Tuning: The Concept

The major objective of the proposed methodology is to facilitate EM-driven antenna optimization processes carried out under challenging scenarios, in particular, the lack of reasonable initial design, or the necessity of re-designing the structure for the operating frequencies/bandwidths that are

severely misaligned with those at the available design. In these and similar situations, local optimizers are prone to a failure, whereas application of global methods (nature-inspired metaheuristics [33], machine learning routines [34], etc.) is usually unjustifiable due to the excessive computational expenses associated with such techniques.

For the sake of explaining the introduced concepts, the design problem is formulated as a minimax task of improving the antenna matching at the target operating bands $[f_{j,1} f_{j,2}]$, $j = 1, \dots, N$, where N is the number of bands, whereas $f_{j,1}$ and $f_{j,2}$ stand for the beginning and the end of the j th band. Denoting the vector of adjustable parameters as \mathbf{x} , we aim at solving

$$\mathbf{x}^* = \arg \min_{\mathbf{x}} U(\mathbf{x}, S_{11}, \mathbf{F}) \quad (1)$$

where $\mathbf{F} = [f_{1,1} f_{1,2} \dots f_{N,1} f_{N,2}]^T$ is the aggregated vector of the target operating bands, whereas the objective function is defined as

$$U(\mathbf{x}, S_{11}, \mathbf{F}) = \max_{j=1, \dots, N} \{f_{j,1} \leq f \leq f_{j,2} : |S_{11}(\mathbf{x}, f)|\} \quad (2)$$

It should be noted that focusing on the reflection characteristic here does not imply any loss of generality because when handling other antenna responses (gain, axial ratio, etc.), the intended operating bandwidth for the latter is strictly correlated with that of the impedance bandwidth (cf. Section III.C). Given the above, the problem (1) is an auxiliary design task, considered for the purpose of design specification management. The primary design task, which may or may not be equivalent to (1), will be defined in Section II.C.

A typical situation has been illustrated in Fig. 1, showing a dual-band antenna optimized for best matching within the target operating bands centered at 3.5 GHz and 5.3 GHz. The design goals are attainable using local search when starting from the design with the response shown using the solid line but not the one represented by the dashed line. This is because the lower resonant frequency at the former initial design is located around 2 GHz, whereas the upper one is closer to 3.5 GHz rather than to 5.3 GHz.

The approach proposed in this paper is to facilitate reliable antenna tuning in situations as described above without resorting to global search routines, and preferably without incurring additional computational expenses (e.g., in the form of multiple local search runs starting from additional initial designs). Toward this end, a design specification management scheme is proposed, in which the target operating frequencies/bandwidths are continuously adjusted during a single algorithm run. The aim is to make sure that the design produced by the previous algorithm iteration is within the region of attraction of the current optimum (i.e., according to the current design specifications).

The proposed concept has been graphically illustrated in Fig. 2. Initially, the specifications are relocated as much as necessary towards the operating frequencies of the antenna at the available initial design so that local optimization can be successful. Subsequently, the specifications are gradually moved towards their original values, and the design follows accordingly. At each stage of the process, the optimum with respect to the current specifications is ensured to be attainable from the currently available parameter set. When close to the

conclusion of the optimization process, the specifications are settled at their original values (Figs. 2(c) and 2(d)).

B. Design Specification Management for Reliable Antenna Tuning: Prerequisites and Acceptance Thresholds

The fundamental issue is the implementation of the design specification management scheme that would allow us to achieve the aforementioned goals. The major tasks are: (i) to quantify the necessary amount of design specification relocation, and (ii) to determine whether the adjusted specs are reachable from the current design (in a local sense). Furthermore, for practical reasons, the realization of these steps should be accomplished at low computational expenses.

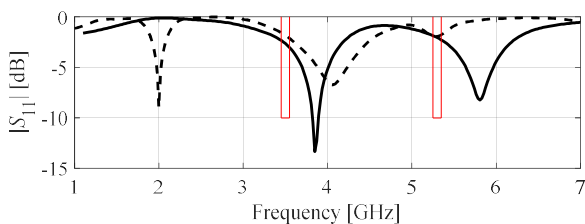


Fig. 1. Exemplary reflection responses of a dual-band antenna with the target operating bandwidths of 3.45-3.55 GHz and 5.25-5.35 GHz marked using vertical lines. The target is attainable from the design featuring the response marked using the solid line, whereas it is not from the design represented by the dashed line, when using local optimization procedures.

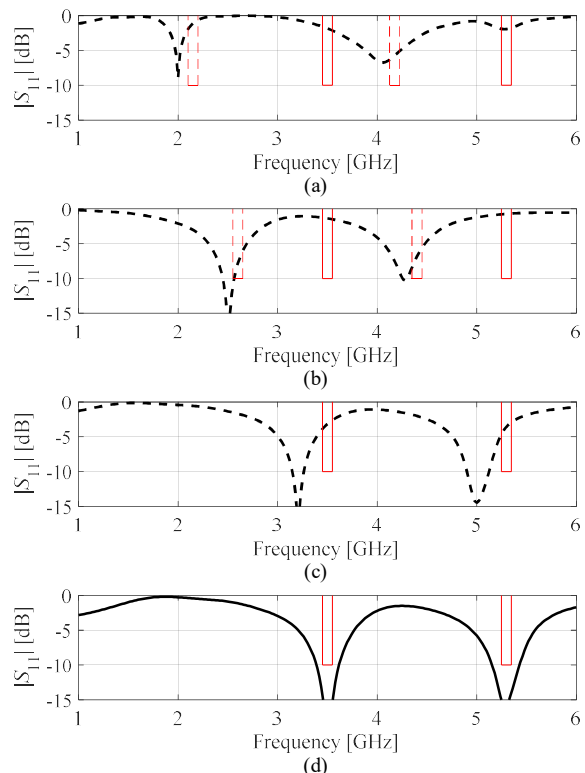


Fig. 2. Conceptual illustration of design specification management approach for reliable optimization of antenna structures. Initial design, and original design specifications (marked using solid lines in all pictures) are the same as in Fig. 1: (a) design specifications shifted towards the initial design resonances to allocate the design within the region of attraction of the optimum w.r.t. the current specs marked using dashed lines; (b) in the middle of the optimization run with current specs adjusted towards the original ones and the design following these; (c) before the last optimization stage: specifications set at their original values; (d) optimization accomplished w.r.t. the original specs.

In this work, the underlying optimization algorithm is assumed to be a trust-region gradient search, therefore, the basic tool utilized to address (i) and (ii) will be a linear model of antenna characteristics established using the known Jacobian matrix. The latter is already available at no extra cost because it needs to be estimated before each iteration of the optimization algorithm.

For the purpose of design specification management, we use the reflection response S_{11} , and denote its gradient at frequency f as $\mathbf{G}_S(\mathbf{x}, f)$. We assume that the optimization algorithm is an iterative procedure that generates a series of approximations $\mathbf{x}^{(i)}$, $i = 0, 1, \dots$, to the optimum design \mathbf{x}^* with $\mathbf{x}^{(0)}$ being the initial design. The linear model $L^{(i)}(\mathbf{x}, f)$ at the current design $\mathbf{x}^{(i)}$ produced by the optimization algorithm takes the form of

$$L^{(i)}(\mathbf{x}, f) = S_{11}(\mathbf{x}^{(i)}, f) + [\mathbf{G}_S(\mathbf{x}^{(i)}, f)]^T (\mathbf{x} - \mathbf{x}^{(i)}) \quad (3)$$

Consider an auxiliary optimization sub-problem

$$\mathbf{x}^{imp} = \arg \min_{\|\mathbf{x} - \mathbf{x}^{(i)}\| \leq D} U(\mathbf{x}, L^{(i)}, \mathbf{F}) \quad (4)$$

where D is the size of the optimization domain (a vicinity of $\mathbf{x}^{(i)}$), typically set to $D = 1$. The decision about whether to adjust the design specifications will be based on the following three factors:

- The improvement factor E_r defined as

$$E_r = |U(\mathbf{x}^{imp}, L^{(i)}, \mathbf{F}) - U(\mathbf{x}^{(i)}, L^{(i)}, \mathbf{F})| \quad (5)$$

- The objective function value at the current iteration point

$$E_0 = U(\mathbf{x}^{(i)}, L^{(i)}, \mathbf{F}) \quad (6)$$

- The distance E_c between the center frequencies of the antenna at $\mathbf{x}^{(i)}$, denoted as $\mathbf{F}_c = [f_{c,1} \dots f_{c,N}]^T$, and the target center frequencies $\mathbf{F}_t = [f_{t,1} \dots f_{t,N}]^T$ with $f_{t,k} = (f_{k,1} + f_{k,2})/2$, $k = 1, \dots, N$, defined as

$$E_c = \|\mathbf{F}_c - \mathbf{F}_t\| \quad (7)$$

The first factor determines the potential for improving the design in terms of the antenna reflection response in the sense of (1), (2), when using $\mathbf{x}^{(i)}$ as a starting point. The second factor evaluates the quality of the design $\mathbf{x}^{(i)}$ in the same sense, whereas the last one will be used as a safeguard to ensure that the updated specifications are sufficiently close to the current operating frequencies of the antenna under design.

Having defined the factors E_r , E_0 , and E_c , as well as the acceptance thresholds $E_{r,\min}$, $E_{0,\max}$, and $E_{c,\max}$, the design requirements are to be adjusted as compared to the original specs \mathbf{F} if

- E_r is too small, $E_r < E_{r,\min}$, i.e., the current design is unlikely to be improved in a sufficient manner from the current point $\mathbf{x}^{(i)}$, or
- E_0 is too large, $E_0 > E_{0,\max}$, i.e., the reflection levels are too high at the current design indicating that the actual operating bands at $\mathbf{x}^{(i)}$ are away from the target, or
- E_c is too large, $E_c > E_{c,\max}$, which is a supplemental way of indicating the same problem as outlined above.

Satisfaction of either of these conditions indicates that the current specifications are too stringent to be attainable from the current design and need to be relaxed. The acceptance threshold values are not critical but they should take into account the antenna

characteristics. A simple procedure for establishing $E_{r,\min}$, $E_{0,\max}$, and $E_{c,\max}$ is the following:

1. Set $E_{c,\max}$ to half of the antenna bandwidth(s) at the initial design, which ensures that the target frequencies will be allocated on the reflection response slopes near the respective resonances or operating bandwidths as long as $E_c < E_{c,\max}$;
2. Temporarily relocate the design specifications (target operating frequencies) so that $E_c = E_{c,\max}$ (cf. (7));
3. Solve sub-problem (4) with $D = 1$;
4. Set $E_{r,\min} = E_r$, with E_r calculated using \mathbf{x}_{imp} obtained in Step 3.

The threshold $E_{r,\min}$ set as above account for a typical objective function improvement when the design specifications are established to satisfy the condition $E_c < E_{c,\max}$. The last acceptance threshold $E_{0,\max}$ is only introduced to handle situations when the antenna characteristics are flat around the target operating frequencies (typically when the reflection level is close to zero), yet the other two conditions are not satisfied. Setting it at certain values below zero dB, allows for distinguishing between such regions, and the situations when the target frequencies are getting closer to the actual operating bandwidths of the antenna. In the numerical experiments of Section III, we set $E_{0,\max} = -2$ dB. It can be observed that the value of D has an immediate effect on the improvement factor E_r , so that changing D would change the number and amount of design specification adjustments in the course of the optimization run. In this work $D = 1$ was chosen to represent an ‘intermediate’ value for typical sizes of microstrip antenna components, normally ranging from fractions of mm to a few dozens of mm.

C. Design Specification Management for Reliable Antenna Tuning: Procedure

Let us denote as $\mathbf{F}_{cr}(a)$ the updated specifications for the next (i.e., $(i+1)$ th) iteration of the optimization algorithm, parameterized by a scalar a , $0 \leq a \leq 1$. They are

$$\mathbf{F}_{cr}(a) = [f_{cr,1.1}(a) f_{cr,1.2}(a) \dots f_{cr,N.1}(a) f_{cr,N.2}(a)]^T \quad (8)$$

where

$$\begin{aligned} f_{cr,k.1}(a) &= f_{cr,k}(a) - B_k(a), \\ f_{cr,k.2}(a) &= f_{cr,k}(a) + B_k(a) \end{aligned} \quad (9)$$

with

$$\begin{aligned} f_{cr,k}(a) &= (1-a)f_{c,k} + af_{t,k}, \\ B_k(a) &= (f_{k.2} - f_{k.1}) \frac{f_{cr,k}(a)}{f_{t,k}} \end{aligned} \quad (10)$$

The coefficient a is the maximum value for which the three conditions $E_r \geq E_{r,\min}$, $E_0 \leq E_{0,\max}$, and $E_c \leq E_{c,\max}$, are satisfied at the design (cf. (4))

$$\mathbf{x}^{imp} = \arg \min_{\|\mathbf{x} - \mathbf{x}^{(i)}\| \leq 1} U(\mathbf{x}, L^{(i)}, \mathbf{F}_{cr}(a)) \quad (11)$$

It should be emphasized that finding the coefficient a as described above is realized by solving a separate optimization sub-problem, in which a is continuously reduced from 1 to zero, until the value is found that ensures satisfaction of the three conditions mentioned above. If this cannot be obtained even

with $a = 0$, the algorithm is terminated as the original specs are considered to be not attainable.

In plain words, the design specifications are relaxed, i.e., the target operating frequencies/bandwidths are relocated towards the antenna center frequencies at the current design, as much as necessary to ensure satisfaction of the three conditions discussed above. Note that the updated k th target center frequency $f_{cr,k}$ is a convex combination of $f_{c,k}$ and the original target center frequency $f_{t,k}$. By reducing a , the specifications are relaxed, which eventually makes our three conditions satisfied. When the current design approaches the optimum, the conditions will be satisfied for $a = 1$, which corresponds to the original specs. This is under the assumption that the specifications are attainable. Otherwise, the optimization process will be terminated upon getting as close to the original specs as possible.

The procedure described in this section is repeated before each iteration of the optimization algorithm, i.e., at all designs $\mathbf{x}^{(i)}$, $i = 0, 1, \dots$. This allows for continuous adjustment of the specifications depending on the relationships between the current design and the original requirements. It should be emphasized that specification adjustment does not incur any computational expenses in terms of EM simulations of the structure at hand because the knowledge of the antenna response and sensitivities is a prerequisite for the optimization algorithm operation (assuming it is a gradient-based routine).

D. Trust-Region Gradient Search

The presented design specification management approach can work with various local iterative search procedures (preferably descent ones). Here, it is demonstrated using the standard trust-region (TR) gradient search [35], which is briefly recalled in this section. The design task is defined as

$$\mathbf{x}^* = \arg \min_{\mathbf{x}} U_R(\mathbf{x}, \mathbf{R}(\mathbf{x}), \mathbf{F}) \quad (12)$$

where \mathbf{R} stand for all relevant antenna responses. The series of approximations $\mathbf{x}^{(i)}$, $i = 0, 1, \dots$, to \mathbf{x}^* (cf. (1)), is produced as

$$\mathbf{x}^{(i+1)} = \arg \min_{\|\mathbf{x} - \mathbf{x}^{(i)}\| \leq d^{(i)}} U_R(\mathbf{x}, L_R^{(i)}, \mathbf{F}_{cr}) \quad (13)$$

where $L_R^{(i)}$ is a linear expansion model of i.e.,

$$L_R^{(i)}(\mathbf{x}, f) = \mathbf{R}(\mathbf{x}^{(i)}, f) + [\mathbf{G}_R(\mathbf{x}^{(i)})]^T (\mathbf{x} - \mathbf{x}^{(i)}) \quad (14)$$

whereas U_R is the objective function pertinent to the design task at hand, and \mathbf{G}_R denotes the response gradient. The trust region radius $d^{(i)}$ is updated after each iteration of the algorithm using the standard TR rules [36]. The antenna response gradients are estimated using finite differentiation.

For the sake of illustration, let us consider maximization of average in-band gain $G(\mathbf{x}, f)$ of the antenna with the constraint imposed on the reflection responses so that $|S_{11}(\mathbf{x}, f)| \leq -10$ dB for $f_{k.1} \leq f \leq f_{k.2}$, $k = 1, \dots, N$. In other words, we require that the function $U(\mathbf{x}, S_{11}, \mathbf{F})$ considered in (2) does not exceed -10 dB. In this case, the objective function may take a form of

$$U_R(\mathbf{x}, \mathbf{R}, \mathbf{F}) = U_R(\mathbf{x}, [G, S_{11}], \mathbf{F}) = -\frac{\sum_{k=1}^N \int_{f_{k,1}}^{f_{k,2}} G(\mathbf{x}, f) df}{\sum_{k=1}^N (f_{k,2} - f_{k,1})} + \beta \left[\max \left\{ \frac{U(\mathbf{x}, S_{11}, \mathbf{F}) + 10}{10}, 0 \right\} \right]^2 \quad (15)$$

The first term in (15) is the average in-band gain to be maximized, whereas the second term is a penalty factor quantifying a relative violation of the reflection constraint.

It should be emphasized that the primary objective function U_R defined for the antenna design purposes, and the auxiliary function U (cf. (1)), are two separate entities, with the former being considered for the purpose of implementing the design specification adjustment as described in Sections II.A through II.C.

E. Optimization Framework

The complete optimization algorithm combines the core optimization routine (here, the TR algorithm outlined in Section II.D), and the design specification management procedure of Section II.C. The specifications are adjusted before each iteration of the algorithm using the auxiliary cost function U . The next iteration point is subsequently found using the primary objective function U_R .

The input parameters of the process are

1. $\mathbf{x}^{(0)}$ – initial design;
2. \mathbf{F} – target operating frequency/band vector;
3. U_R – primary objective function encoding design goals;

The operating flow of the algorithm is the following:

1. Set the iteration index $i = 0$;
2. Find the scalar a to determine current specification vector $\mathbf{F}_{cr}(a)$ (cf. Section II.C); if the conditions $E_r \geq E_{r,\min}$, $E_0 \leq E_{0,\max}$, and $E_c \leq E_{c,\max}$, cannot be satisfied even for $a = 0$, go to 7 (premature termination).
3. Perform TR iteration (13) to find the new iteration point $\mathbf{x}^{(i+1)}$ according to \mathbf{F}_{cr} ;
4. Update the TR radius $d^{(i)}$;
5. If the termination condition is satisfied, go to 7;
6. **If** $U_R(\mathbf{x}^{(i+1)}, \mathbf{R}(\mathbf{x}^{(i+1)}), \mathbf{F}_{cr}) < U_R(\mathbf{x}^{(i)}, \mathbf{R}(\mathbf{x}^{(i)}), \mathbf{F}_{cr})$
 Set $i = i + 1$;
 Go to 2;
 else
 Go to 3;
 end
7. END

The termination condition is based on the convergence in argument $\|\mathbf{x}^{(i+1)} - \mathbf{x}^{(i)}\| < \varepsilon$, or reduction of the TR radius $d^{(i)} < \varepsilon$. In our numerical experiments, we use $\varepsilon = 10^{-3}$. Note that if no improvement of the primary objective function is observed (Step 6), the new point is rejected and the iteration is repeated with a reduced TR radius. More details concerning trust-region algorithms can be found in [36]. For the sake of additional clarification, Fig. 3 shows the flow diagram of the procedure.

III. VERIFICATION CASE STUDIES

This section demonstrates the operation of the optimization framework introduced in Section II with the emphasis on the benefits of design specification management, and its role in handling challenging design scenarios that involve poor starting points. We consider three antenna structures, uniplanar dipoles (a dual- and a triple-band), as well as a quasi-Yagi antenna optimized for maximum in-band gain.

Experimental validation of the designs pertinent to the considered benchmark structures is not considered because this work is not concerned with the design of novel antenna structures but it is oriented towards the development of the optimization procedures. All antennas have been taken from the literature as verification cases and have already been validated both in the source papers (e.g., [37], [39]), and in the context of numerical optimization (e.g., [40], [41]). Given the focus and the scope of this work, numerical results are more than sufficient to support the conclusions of the paper as elaborated on in Section IV.

A. Case 1: Dual-Band Dipole

Consider a coplanar-waveguide-fed uniplanar dual-band dipole antenna shown in Fig. 4 [37], implemented on the RO4350 substrate ($\varepsilon_r = 3.48$, $h = 0.762$ mm). The antenna geometry is described by six parameters $\mathbf{x} = [l_1 \ l_2 \ l_3 \ w_1 \ w_2 \ w_3]^T$; $l_0 = 30$, $w_0 = 3$, $s_0 = 0.18$, and $o = 5$ are fixed (all dimensions in mm). The EM model is implemented in CST Microwave Studio, and evaluated using the time-domain solver.

The design task is to improve antenna matching at the ± 50 MHz bands centered at 3.5 GHz and 5.3 GHz. Thus, the target operating frequency vector is $\mathbf{F} = [3.45 \ 3.55 \ 5.25 \ 5.35]^T$ GHz. The initial design shown in Fig. 5 using a dashed line, has been selected to illustrate the efficacy of the proposed design specification adaptation procedure. Local search starting from this $\mathbf{x}^{(0)} = [36.0 \ 7.0 \ 21.0 \ 0.6 \ 5.0 \ 4.5]^T$ fails to find a satisfactory design because of significant misalignment between the center frequencies at $\mathbf{x}^{(0)}$ and the targets; the obtained design is $\mathbf{x}^{conv} = [36.7 \ 7.7 \ 15.3 \ 0.29 \ 5.0 \ 1.86]^T$. Notwithstanding, the procedure of Section II is capable of identifying the optimum, $\mathbf{x}^* = [29.9 \ 15.9 \ 22.6 \ 0.55 \ 1.65 \ 1.91]^T$ mm, marked using the solid line in Fig. 5, without any problems. The overall optimization cost if 106 EM simulations of the antenna structure, including finite differentiation for gradient estimation. Figure 6 shows the evolution of the design specifications in terms of the target center frequencies. It can be observed that the design targets are relocated towards lower frequencies, i.e., into the vicinity of the resonances of the antenna at the initial design. In later iterations, as the design gets closer to the original targets, the specifications are adjusted accordingly. After seven iterations, the specifications are already at their original values, yet the optimization process continues because relocating resonances has to be followed by improving antenna reflection therein as much as possible, according to the assumed objective function. Figure 7 illustrates this for selected intermediate designs rendered in the course of the optimization run.

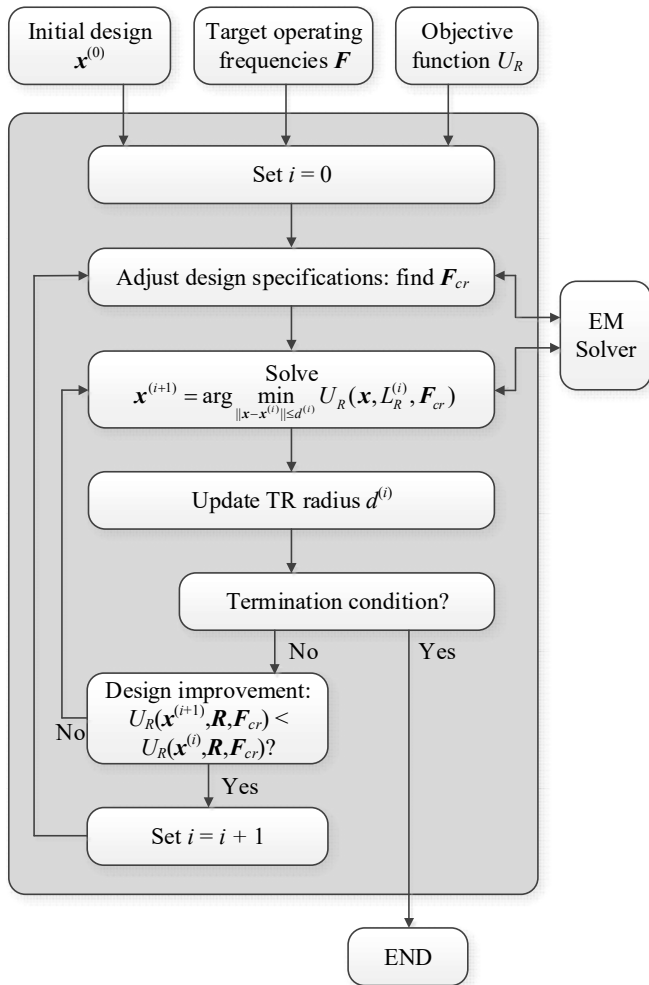


Fig. 3. Flow diagram of the proposed optimization framework with design specification management.

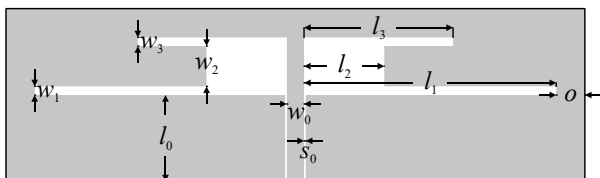


Fig. 4. Dual-band dipole antenna: geometry [37].

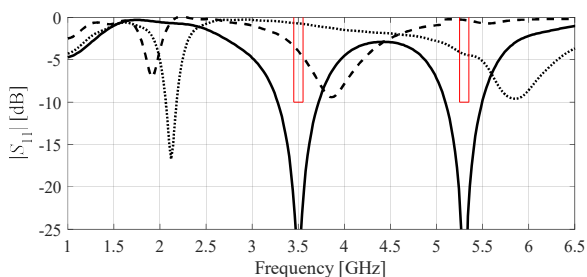


Fig. 5. Dual-band antenna: reflection response at the initial (---) and the final design (—) obtained using the proposed design specification adaptation approach; a dotted line represents the design obtained using conventional local search. Design specifications marked using the thin solid lines.

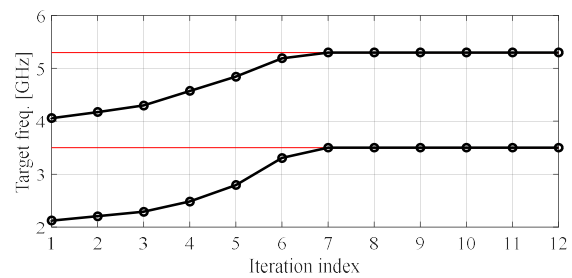


Fig. 6. Dual-band antenna: evolution of the target operating frequencies versus iteration index of the optimization algorithm. Original specifications marked using horizontal lines.

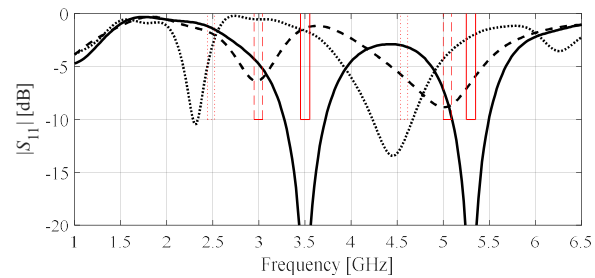


Fig. 7. Dual-band antenna: antenna responses at two intermediate designs, marked using the dotted and dashed lines, as well as the optimum (solid line), along with the corresponding design targets.

B. Case 2: Triple-Band Dipole

Our second example is the triple-band dipole antenna [38], also implemented on the RO4350 substrate. The structure, shown in Fig. 8, is described by ten parameters $\mathbf{x} = [l_1 \ l_2 \ l_3 \ l_4 \ l_5 \ w_1 \ w_2 \ w_3 \ w_4 \ w_5]^T$; $l_0 = 30$, $w_0 = 3$, $s_0 = 0.15$, and $o = 5$ are fixed (dimensions in mm). The computational model is implemented in CST. The design task is to improve antenna matching at the ± 50 MHz bands centered at 2.45 GHz, 3.6 GHz, and 5.3 GHz. Thus, the target operating frequency vector is $\mathbf{F} = [2.40 \ 2.50 \ 3.55 \ 3.65 \ 5.25 \ 5.35]^T$ GHz.

Similarly as before, the initial design (dashed line in Fig. 9) has been selected to demonstrate the robustness of the proposed approach. Conventional local optimization fails to identify the optimum design for the same reason as in the previous example: severe misalignment between the center frequencies at $\mathbf{x}^{(0)} = [39.9 \ 9.42 \ 30.0 \ 9.69 \ 20.9 \ 2.2 \ 4.2 \ 0.62 \ 0.38 \ 2.00]^T$ and the targets. The design obtained through local search is $\mathbf{x}^{conv} = [34.3 \ 5.0 \ 30.0 \ 13.3 \ 21.0 \ 1.98 \ 3.98 \ 2.2 \ 1.90 \ 0.66]^T$. On the other hand, the framework proposed in this work is capable of finding the high-quality design $\mathbf{x}^* = [37.1 \ 12.7 \ 27.3 \ 10.9 \ 19.7 \ 1.24 \ 2.37 \ 1.30 \ 0.37 \ 0.58]^T$ mm (cf. Fig. 8, solid line). The overall optimization cost is 178 EM simulations of the antenna structure, including finite differentiation for gradient estimation.

The evolution of the target center frequencies as a function of the algorithm iteration has been shown in Fig. 10, indicating the same qualitative behavior as for the first test antenna. Following the heavy initial modifications, the target frequencies converge to their original values within the first nine iterations of the optimization process. For the sake of supplementary illustration Fig. 11 depicts the selected intermediate designs, and the corresponding specifications encountered during the optimization run.

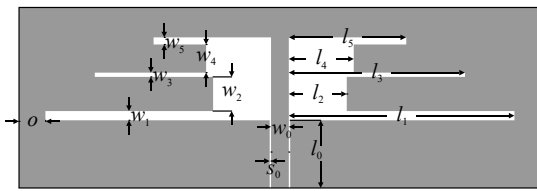


Fig. 8. Triple-band dipole antenna: geometry [38].

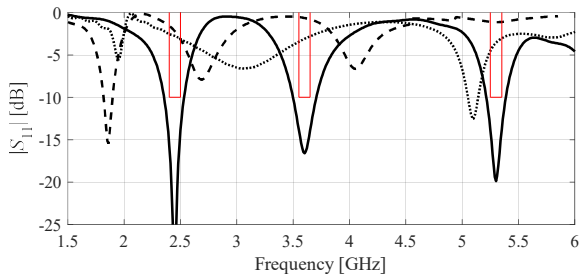


Fig. 9. Triple-band antenna: reflection response at the initial (- -) and the final design (-) obtained using the proposed design specification adaptation approach; a dotted line represents the design obtained using conventional local search. Design specifications marked using the thin solid lines.

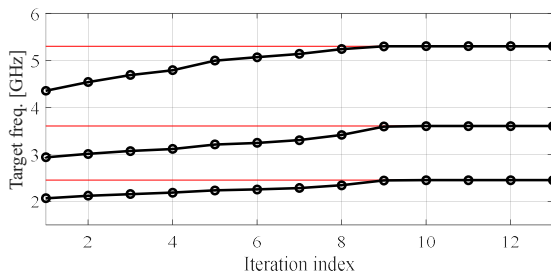


Fig. 10. Triple-band antenna: evolution of the target operating frequencies versus iteration index of the optimization algorithm. Original specifications marked using horizontal lines.

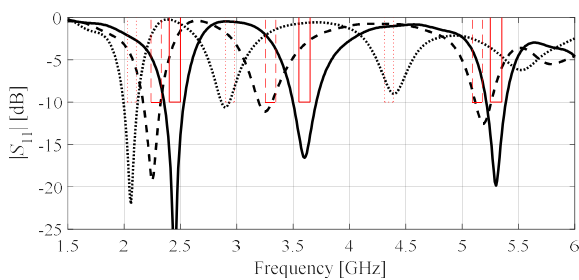


Fig. 11. Triple-band antenna: antenna responses at two intermediate designs, marked using the dotted and dashed lines, as well as the optimum (solid line), along with the corresponding design targets.

C. Case 3: Quasi-Yagi Antenna

The last verification example is a quasi-Yagi antenna with a parabolic reflector (Fig. 12) [39], implemented on FR4 dielectric substrate ($\epsilon_r = 4.4$, $h = 1.5$). The EM model is simulated in CST. The geometry parameters are $\mathbf{x} = [W L L_m L_p S_d S_r W_2 W_a W_d g]^T$ (all dimensions in mm). The feed line width $W_1 = 3.0$ is set to ensure 50-ohm input impedance.

The design task is to maximize the average realized gain within the ± 200 MHz frequency range centered at 4.8 GHz. At the same time, the antenna reflection is supposed not to exceed -10 dB within the same bandwidth. Thus, in this case, the target

operating frequency vector is $\mathbf{F} = [4.60 \ 5.00]^T$ GHz. The primary objective function is defined as in (15) with the penalty factor $\beta = 10$.

The initial design $\mathbf{x}^{(0)}$ shown in Fig. 13 using the dashed line has been selected away from the target bandwidth to ensure that the optimization process is sufficiently challenging. The standard local optimization process expectedly fails when starting from $\mathbf{x}^{(0)} = [130.0 \ 68.0 \ 22.1 \ 20.0 \ 0.60 \ 17.3 \ 3.95 \ 11.0 \ 23.2 \ 0.5]^T$. The design obtained through local search is $\mathbf{x}^{conv} = [149.4 \ 78.5 \ 29.3 \ 26.4 \ 0.9 \ 13.5 \ 3.46 \ 9.9 \ 15.3 \ 0.57]^T$. The proposed approach yields the optimum designs also shown in Fig. 13 using the solid line, $\mathbf{x}^* = [118.6 \ 62.2 \ 35.0 \ 24.1 \ 0.89 \ 9.5 \ 2.00 \ 9.12 \ 19.0 \ 0.99]^T$ mm. The overall optimization cost is 118 EM simulations of the antenna structure, including finite differentiation for gradient estimation. Figures 14 and 15 show the evolution of the target center frequency, as well as the antenna responses at the selected intermediate designs along with the corresponding specifications. The overall performance of the algorithm is consistent with what was observed for the first two verification cases.

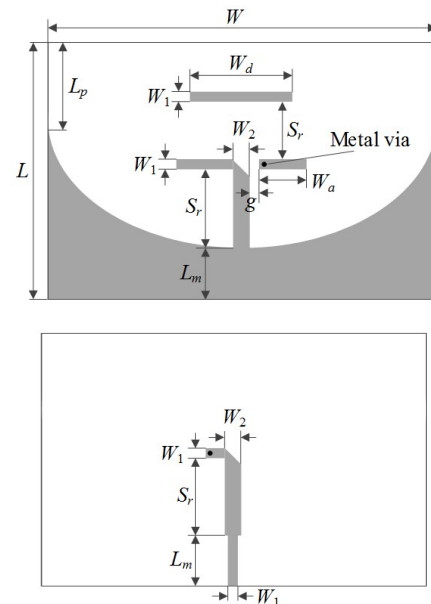


Fig. 12. Planar quasi-Yagi antenna: geometry [39]; top layer (top), bottom layer (bottom).

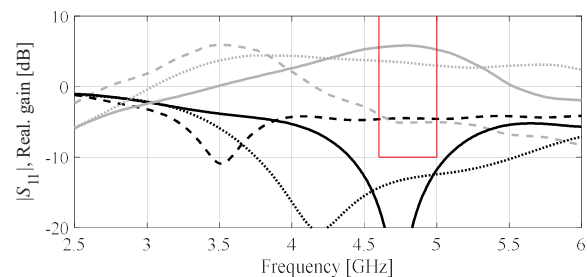


Fig. 13. Quasi-Yagi antenna: reflection response at the initial (- -) and the final design (-) obtained using the proposed design specification adaptation approach; dotted lines represent the design obtained using conventional local search. Design specifications marked using the thin solid lines. Reflection and realized gain characteristics marked using black and gray curves, respectively.

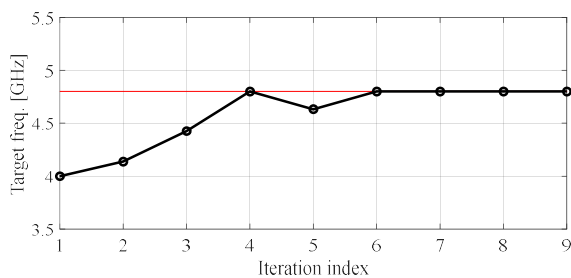


Fig. 14. Quasi-Yagi antenna: evolution of the target operating frequency versus iteration index of the optimization algorithm. Original specifications marked using horizontal lines.

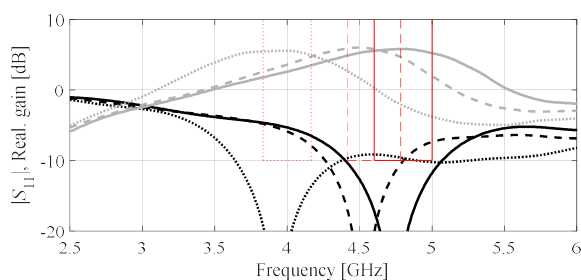


Fig. 15. Quasi-Yagi antenna: antenna responses at two intermediate designs, marked using the dotted and dashed lines, as well as the optimum (solid line), along with the corresponding design targets. Reflection and realized gain characteristics marked using black and gray curves, respectively.

IV. CONCLUSION

This paper proposed a novel approach to design optimization of antenna structures, aiming at the improvement of the reliability and robustness of the parameter tuning process. In pursuit of this goal, a design specification management procedure was introduced, which is intended to work with local search procedures. Here, it is coupled with the trust-region gradient routine. Our methodology allows for relocating the design specifications depending on the quality of the initial point (as well as all intermediate designs along the optimization path), so as the adjusted targets become attainable through the local search. In the course of the algorithm run, the specifications gradually converge to their original levels. The presented technique has been demonstrated to greatly improve the reliability of the search process even if the initial designs are of poor quality with the antenna operating frequencies/bandwidths significantly misaligned with respect to the assumed targets. The major advantages of the proposed framework include reducing the sensitivity of the optimization process to the initial design quality, as well as enabling antenna dimension scaling in broad ranges of operating frequencies using local algorithms. Additional benefits are eliminating the need for employing costly global search routines, or other sophisticated algorithmic solutions (e.g., surrogate modeling or machine learning methods).

ACKNOWLEDGMENT

The authors would like to thank Dassault Systemes, France, for making CST Microwave Studio available.

REFERENCES

- [1] K. Wong, H. Chang, J. Chen, and K. Wang, "Three wideband monopolar patch antennas in a Y-shape structure for 5G multi-input-multi-output access points," *IEEE Ant. Wireless Prop. Lett.*, vol. 19, no. 3, pp. 393-397, 2020.
- [2] A. T. Mobashsher, K. S. Bialkowski, and A. M. Abbosh, "Design of compact cross-fed three-dimensional slot-loaded antenna and its application in wideband head imaging system," *IEEE Ant. Wireless Prop. Lett.*, vol. 15, pp. 1856-1860, 2016.
- [3] Y. Wang, J. Zhang, F. Peng, and S. Wu, "A glasses frame antenna for the applications in internet of things," *IEEE Internet of Things J.*, vol. 6, no. 5, pp. 8911-8918, 2019.
- [4] G. Gao, C. Yang, B. Hu, R. Zhang, and S. Wang, "A wearable PIFA with an all-textile metasurface for 5 GHz WBAN applications," *IEEE Ant. Wireless Prop. Lett.*, vol. 18, no. 2, pp. 288-292, 2019.
- [5] L. Dang, Z. Y. Lei, Y. J. Xie, G. L. Ning, and J. Fan, "A compact microstrip slot triple-band antenna for WLAN/wimax applications," *IEEE Ant. Wireless Prop. Lett.*, vol. 9, pp. 1178-1181, 2010.
- [6] P. Kumar, S. Dwari, R. K. Saini, and M. K. Mandal, "Dual-band dual-sense polarization reconfigurable circularly polarized antenna," *IEEE Ant. Wireless Prop. Lett.*, vol. 18, no. 1, pp. 64-68, 2019.
- [7] Y. Xu, J. Wang, L. Ge, X. Wang, and W. Wu, "Design of a notched-band vivaldi antenna with high selectivity," *IEEE Ant. Wireless Prop. Lett.*, vol. 17, no. 1, pp. 62-65, 2018.
- [8] H. Deng, T. Xu, Y. Xue, F. Liu, and L. Sun, "closely spaced broadband MIMO differential filtering slotline antenna with CM suppression," *IEEE Ant. Wireless Prop. Lett.*, vol. 17, no. 12, pp. 2498-2502, 2018.
- [9] A. Narbudowicz, M. J. Ammann, and D. Heberling, "Reconfigurable axial ratio in compact GNSS antennas," *IEEE Trans. Ant. Propag.*, vol. 64, no. 10, pp. 4530-4533, 2016.
- [10] Y. Liu, S. Wang, X. Wang, and Y. Jia, "A differentially fed dual-polarized slot antenna with high isolation and low profile for base station application," *IEEE Ant. Wireless Prop. Lett.*, vol. 18, no. 2, pp. 303-307, 2019.
- [11] Q. Chen, J. Li, G. Yang, B. Cao, and Z. Zhang, "A polarization-reconfigurable high-gain microstrip antenna," *IEEE Trans. Ant. Propag.*, vol. 67, no. 5, pp. 3461-3466, 2019.
- [12] Z. Liang, S. Lv, Y. Li, J. Liu, and Y. Long, "Compact folded slot antenna and its endfire arrays with high gain and vertical polarization," *IEEE Ant. Wireless Prop. Lett.*, vol. 19, no. 5, pp. 786-790, 2020.
- [13] E. Hassan, D. Noreland, R. Augustine, E. Wadbro, and M. Berggren, "Topology optimization of planar antennas for wideband near-field coupling," *IEEE Trans. Ant. Propag.*, vol. 63, no. 9, pp. 4208-4213, 2015.
- [14] S. Koziel and A. Pietrenko-Dabrowska, "Expedited feature-based quasi-global optimization of multi-band antennas with Jacobian variability tracking," *IEEE Access*, vol. 8, pp. 83907-83915, 2020.
- [15] S. Koziel and S. Ogurtsov, *Antenna design by simulation-driven optimization. Surrogate-based approach*, Springer, New York, 2014.
- [16] S. Koziel and S. Ogurtsov, *Simulation-based optimization of antenna arrays*, World Scientific, Singapore, 2019.
- [17] J. C. Cervantes-González, J. E. Rayas-Sánchez, C. A. López, J. R. Camacho-Pérez, Z. Brito-Brito, and J. L. Chávez-Hurtado, "Space mapping optimization of handset antennas considering EM effects of mobile phone components and human body," *Int. J. RF Microwave CAE*, vol. 26, no. 2, pp. 121-128, 2016.
- [18] S. Koziel and S.D. Uunnsteinsson "Expedited design closure of antennas by means of trust-region-based adaptive response scaling," *IEEE Antennas Wireless Prop. Lett.*, vol. 17, no. 6, pp. 1099-1103, 2018.
- [19] C. Zhang, F. Feng, V. Gongal-Reddy, Q. J. Zhang, and J. W. Bandler, "Cognition-driven formulation of space mapping for equal-ripple optimization of microwave filters," in *IEEE Trans. Microwave Theory Techn.*, vol. 63, no. 7, pp. 2154-2165, 2015.
- [20] J.A. Easum, J. Nagar, P.L. Werner, and D.H. Werner, "Efficient multi-objective antenna optimization with tolerance analysis through the use of surrogate models," *IEEE Trans. Ant. Propag.*, vol. 66, no. 12, pp. 6706-6715, 2018.
- [21] D.I.L. de Villiers, I. Couckuyt, and T. Dhaene, "Multi-objective optimization of reflector antennas using kriging and probability of

- improvement," *Int. Symp. Ant. Prop.*, pp. 985-986, San Diego, USA, 2017.
- [22] A.K.S.O. Hassan, A.S. Etman, and E.A. Soliman, "Optimization of a novel nano antenna with two radiation modes using kriging surrogate models," *IEEE Photonic J.*, vol. 10, no. 4, art. no. 4800807, 2018.
- [23] J. Cai, J. King, C. Yu, J. Liu, and L. Sun, "Support vector regression-based behavioral modeling technique for RF power transistors," *IEEE Microwave and Wireless Comp. Lett.*, vol. 28, no. 5, pp. 428-430, 2018.
- [24] J. Tak, A. Kantemur, Y. Sharma, and H. Xin, "A 3-D-printed W-band slotted waveguide array antenna optimized using machine learning," *IEEE Ant. Wireless Prop. Lett.*, vol. 17, no. 11, pp. 2008-2012, 2018.
- [25] Q. Wu, H. Wang, and W. Hong, "Multistage collaborative machine learning and its application to antenna modeling and optimization," *IEEE Trans. Ant. Propag.*, vol. 68, no. 5, pp. 3397-3409, 2020.
- [26] S. Koziel, A. Bekasiewicz, I. Couckuyt, and T. Dhaene, "Efficient multi-objective simulation-driven antenna design using co-kriging," *IEEE Trans. Antennas Prop.*, vol. 62, no. 11, pp. 5900-5905, 2014.
- [27] B. Liu, S. Koziel, and N. Ali, "SADEA-II: a generalized method for efficient global optimization of antenna design," *J. Comp. Design Eng.*, vol. 4, no. 2, pp. 86-97, 2017.
- [28] Y. Sharma, H. H. Zhang, and H. Xin, "Machine learning techniques for optimizing design of double T-shaped monopole antenna," *IEEE Trans. Ant. Propag.*, vol. 68, no. 7, pp. 5658-5663, 2020.
- [29] C. Cui, Y. Jiao, and L. Zhang, "Synthesis of some low sidelobe linear arrays using hybrid differential evolution algorithm integrated with convex programming," *IEEE Ant. Wireless Prop. Lett.*, vol. 16, pp. 2444-2448, 2017.
- [30] J. Tak, A. Kantemur, Y. Sharma, and H. Xin, "A 3-D-printed W-band slotted waveguide array antenna optimized using machine learning," *IEEE Ant. Wireless Prop. Lett.*, vol. 17, no. 11, pp. 2008-2012, 2018.
- [31] Z. Lv, L. Wang, Z. Han, J. Zhao, and W. Wang, "Surrogate-assisted particle swarm optimization algorithm with Pareto active learning for expensive multi-objective optimization," *IEEE/CAA J. Automatica Sinica*, vol. 6, no. 3, pp. 838-849, 2019.
- [32] D. K. Lim, D. K. Woo, H. K. Yeo, S. Y. Jung, J. S. Ro, and H. K. Jung, "A novel surrogate-assisted multi-objective optimization algorithm for an electromagnetic machine design," *IEEE Trans. Magn.*, vol. 51, no. 3, paper 8200804, 2015.
- [33] A. Lalbakhsh, M.U. Afzal, and K. Esselle, "Multiobjective particle swarm optimization to design a time-delay equalizer metasurface for an electromagnetic band-gap resonator antenna," *IEEE Ant. Wireless Propag. Lett.*, vol. 16, pp. 912-915, 2017.
- [34] S. Jeong, J. G. D. Hester, W. Su, and M. M. Tentzeris, "Read/interrogation enhancement of chipless RFIDs using machine learning techniques," *IEEE Ant. Wireless Propag. Lett.*, vol. 18, no. 11, pp. 2272-2276, 2019.
- [35] A. Pietrenko-Dabrowska and S. Koziel, "Computationally-efficient design optimization of antennas by accelerated gradient search with sensitivity and design change monitoring," *IET Microwaves Ant. Prop.*, vol. 14, no. 2, pp. 165-170, 2020.
- [36] A.R. Conn, N.I.M. Gould, and P.L. Toint, *Trust Region Methods*, MPS-SIAM Series on Optimization, 2000.
- [37] Y.-C. Chen, S.-Y. Chen, and P. Hsu, "Dual-band slot dipole antenna fed by a coplanar waveguide," in *Proc. IEEE Ant. Propag. Society Int. Symp.*, Albuquerque, NM, USA, 2006, pp. 3589-3592.
- [38] A. Pietrenko-Dabrowska, S. Koziel, and M. Al-Hasan, "Expedited yield optimization of narrow- and multi-band antennas using performance-driven surrogates," *IEEE Access*, pp. 143104-143113, 2020.
- [39] Z. Hua, G. Haichuan, L. Hongmei, L. Beijia, L. Guanjun, and W. Qun, "A novel high-gain quasi-Yagi antenna with a parabolic reflector," *Int. Symp. Ant. Prop. (ISAP)*, Hobart, Australia, 2015.
- [40] S. Koziel, and A. Bekasiewicz, "Fast re-design and geometry scaling of multi-band antennas using inverse surrogate modeling techniques," *Int. J. Numerical Modeling*, vol. 31, no. 3, 2018.
- [41] S. Koziel and A. Pietrenko-Dabrowska, "Kriging metamodels and design re-utilization for fast parameter tuning of antenna structures," *Int. J. Numerical Modeling*, art. no. e02811, 2020.



SLAWOMIR KOZIEL received the M.Sc. and Ph.D. degrees in electronic engineering from Gdansk University of Technology, Poland, in 1995 and 2000, respectively. He also received the M.Sc. degrees in theoretical physics and in mathematics, in 2000 and 2002, respectively, as well as the PhD in mathematics in 2003, from the University of Gdansk, Poland. He is currently a Professor with the Department of Engineering, Reykjavik University, Iceland. His research interests include CAD and modeling of microwave and antenna structures, simulation-driven design, surrogate-based optimization, space mapping, circuit theory, analog signal processing, evolutionary computation and numerical analysis.



ANNA PIETRENKO-DABROWSKA received the M.Sc. and Ph.D. degrees in electronic engineering from Gdansk University of Technology, Poland, in 1998 and 2007, respectively. Currently, she is an Associate Professor with Gdansk University of Technology, Poland. Her research interests include simulation-driven design, design optimization, control theory, modeling of microwave and antenna structures, numerical analysis.